CHEMISTRY
A EUROPEAN JOURNAL

DOI: 10.1002/chem.200800998

Comparison of the Surprising Metal-Ion-Binding Properties of 5- and 6-Uracilmethylphosphonate ($5Umpa^{2-}$ and $6Umpa^{2-}$) in Aqueous Solution and Crystal Structures of the Dimethyl and Di(isopropyl) Esters of $H_2(6Umpa)$**

Eva Freisinger,*[a] Rolf Griesser,[b] Bernhard Lippert,[c] Cristóbal F. Moreno-Luque,[b, d] Juan Niclós-Gutiérrez,[d] Justyn Ochocki,[e] Bert P. Operschall,[b] and Helmut Sigel*[b]

Dedicated with best wishes to Professor Jan Reedijk on the occasion of his 65th birthday

Abstract: 5- and 6-Uracilmethylphosphonate ($5Umpa^{2-}$ and $6Umpa^{2-}$) as acyclic nucleotide analogues are in the focus of anticancer and antiviral research. Connected metabolic reactions involve metal ions; therefore, we determined the stability constants of M(Umpa) complexes ($M^{2+} = Mg^{2+}$, Ca^{2+}, Mn^{2+}, Co^{2+}, Cu^{2+}, Zn^{2+}, or Cd^{2+}). However, the coordination chemistry of these Umpa species is also of interest in its own right, for example, the phosphonate-coordinated M^{2+} interacts with (C4)O to form seven-membered chelates with $5Umpa^{2-}$, thus leading to intramolecular equilibria between open (op) and closed (cl) isomers. No such interaction occurs with $6Umpa^{2-}$. In both M(Umpa) series deprotonation of the uracil residue leads to the formation of $M(Umpa-H)^-$ complexes at higher pH values. Their stability was evaluated by taking into account the fact that the uracilate residue can bind metal ions to give $M_2(Umpa-H)^+$ species. This has led to two further important insights: 1) In $M(6Umpa-H)^-_{cl}$ the H^+ is released from (N1)H, giving rise to six-membered chelates (degrees of formation of ca. 90 to 99.9% with Mn^{2+}, Co^{2+}, Cu^{2+}, Zn^{2+}, or Cd^{2+}). 2) In $M(5Umpa-H)^-_{cl}$ the (N3)H is deprotonated, leading to a higher stability of the seven-membered chelates involving (C4)O (even Mg^{2+} and Ca^{2+} chelates are formed up to ≈50%). In both instances the $M(Umpa-H)^-_{op}$ species led to the formation of $M_2(Umpa-H)^+$ complexes that have one M^{2+} at the phosphonate and one at the $(N3)^-$ (plus carbonyl) site; this proves that nucleotides can bind metal ions independently at the phosphate and the nucleobase residues. X-ray structural analyses of 6Umpa derivatives show that in diesters the phosphonate group is turned away from the uracil residue, whereas in $H_2(6Umpa)$ the orientation is such that upon deprotonation in aqueous solution a strong hydrogen bond is formed between (N1)H and PO_3^{2-}; replacement of the hydrogen with M^{2+} gives the $M(6Umpa-H)^-_{cl}$ chelates mentioned.

Keywords: chelates · equilibrium constants · isomeric equilibria · metal–ion binding · nucleotide analogues · transition metals

[a] Prof. E. Freisinger
Institute of Inorganic Chemistry, University of Zürich
8057 Zürich (Switzerland)
Fax: (+41) 44-635-6802
E-mail: freisinger@aci.uzh.ch

[b] Dr. R. Griesser, Dr. C. F. Moreno-Luque, Dipl.-Ing. B. P. Operschall, Prof. H. Sigel
Department of Chemistry, Inorganic Chemistry
University of Basel, 4056 Basel (Switzerland)
Fax: (+41) 61-267-1017
E-mail: Helmut.Sigel@unibas.ch

[c] Prof. B. Lippert
Department of Chemistry, Technische Universität Dortmund
44227 Dortmund (Germany)

[d] Dr. C. F. Moreno-Luque, Prof. J. Niclós-Gutiérrez
Department of Inorganic Chemistry, Faculty of Pharmacy
University of Granada, 18071 Granada (Spain)

[e] Prof. J. Ochocki
Department of Bioinorganic Chemistry
Faculty of Pharmacy, Medical University
90-151 Łódź (Poland)

[**] The IUPAC names of $5Umpa^{2-}$ and $6Umpa^{2-}$ are uracil-5-ylmethylphosphonate and uracil-6-ylmethylphosphonate, respectively.

1. Introduction

Many phosphonate derivatives possess biological activities, especially those considered to be nucleotide analogues,[1,2] such as 5- and 6-uracilmethylphosphonate (5Umpa^{2-} and 6Umpa^{2-}; Figure 1), which significantly prolong the survival

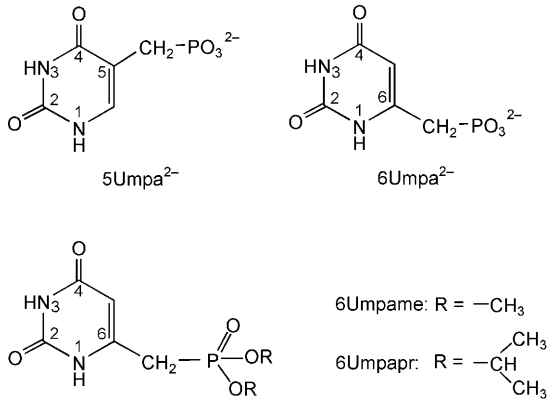

Figure 1. Chemical structures of 5- (5Umpa^{2-}) and 6-uracilmethylphosphonate (6Umpa^{2-}) as well as those of the two esters dimethyl 6-uracilmethylphosphonate (6Umpame) and di(isopropyl) 6-uracilmethylphosphonate (6Umpapr). For comparison, the two simple nucleobase derivatives 5-methyuracil (5MeUr = thymine) and 6-methyluracil (6MeUr) are also considered in this study. The (N3)H (or (N1)H) deprotonated species of Umpa^{2-} are abbreviated as (Umpa−H)$^{3-}$ and should be read as Umpa minus H$^+$.

time of mice with lymphoid leukemia L-1210, also as the dimethyl esters, if administered in combination with cisplatin.[3] Similarly, Na$^+$, K$^+$/5Umpa^{2-}, and some diester derivatives inhibit the growth of human peripheral blood lymphocytes as well as colon adenocarcinoma cell lines HT 29.[4]

Within the large group of acyclic nucleotide analogues, 9-[2-(phosphonomethoxy)ethyl]adenine (PMEA),[2] also known as Adefovir,[5] turned out to be an especially successful compound; it is active against a wide range of viruses, including herpes viruses, poxviruses, hepadnaviruses, and retroviruses, and it also has antineoplastic and immunomodulatory activities.[5] In its oral prodrug form, that is, its bis(pivaloyloxymethyl)ester (Adefovir dipivoxil or Hepsera), it is now on the market[6,7] for the treatment of hepatitis B patients infected with the HB DNA virus. In the cell the dianion of PMEA is diphosphorylated by kinases[5,8] to become a triphosphate analogue that is initially recognized by nucleic acid polymerases as a substrate; thus giving rise to its biological action.[1,2]

Because, as indicated above, neutral diesters are employed as prodrugs, which allows easier passage through cell membranes,[9,10] and because kinases and nucleic acid polymerases depend on metal ions for their activity,[1] we have now partially studied both aspects with 5Umpa and 6Umpa (Figure 1). First, the dimethyl and di(isopropyl) esters of 6Umpa could be crystallized and their solid-state structures compared with that of the parent acid, H_2(6Umpa).[12] Second, for Mg^{2+}, Ca^{2+}, Mn^{2+}, Co^{2+}, Cu^{2+}, Zn^{2+}, and Cd^{2+}, the M^{2+} binding properties in aqueous solution were determined by potentiometric pH titrations for 5Umpa^{2-} and 6Umpa^{2-} and it could be shown that the coordination chemistry of these two isomeric uracil derivatives (Figure 1) differs considerably. For example, with M(5Umpa), seven-membered chelates form by the interaction of the phosphonate-coordinated M^{2+} ion with the carbonyl oxygen (C4)O, whereas in the M(6Umpa) species only phosphonate binding occurs; however, upon uracil deprotonation rather stable chelates form with (N1)$^-$. Furthermore, in both series M_2(Umpa−H)$^+$ species exist.

2. Results and Discussion

2.1. Crystal structures of the dimethyl and di(isopropyl) esters of 6Umpa: The solid-state structures of the neutral 6Umpame and 6Umpapr diesters, together with H_2(6Umpa),[12] are shown in Figure 2. The geometry of the uracil moiety is in the normal range in all instances.

Although the overall orientation of the methylphosphonate entities would be, in principle, favorable for the formation of intramolecular hydrogen bonds between (N1)H of the uracil moieties and the phosphonic acid residues, the observed distances in the solid-state structures of 6Umpame, 6Umpapr, and H_2(6Umpa) are too long and the angles involving the (N1)H proton deviate considerably from 180° (6Umpame: N1···O13 3.627(5) Å, (N1)H···O13 3.69(3) Å, N1−H···O13 78.8(3)°; 6Umpapr: N1···O14 3.196(3) Å, (N1)H···O14 2.98(3) Å, N1−H···O14 96.5(3)°; H_2(6Umpa):[12] N1···O13 3.158(3) Å, (N1)H···O13 2.83(3) Å, N1-H···O13 99.8(3)°]. As in H_2(6Umpa), intramolecular hydrogen bonding in 6Umpame and 6Umpapr might be impeded by the formation of more favorable intermolecular hydrogen bonds involving the (N1)H proton, as described below. However, in aqueous solution the formation of a rather strong hydrogen bond between (N1)H and PO_3^{2-} could be proven upon deprotonation of the $PO(OH)_2$ group.[12]

With 6Umpame the molecules form infinite chains in a zigzag arrangement along the x axis with one hydrogen bond each between neighboring nucleobases (N3···O4 ($0.5+x$, y, $0.5-z$) and O4···N3 ($-0.5+x$, y, $0.5-z$) 2.893(4) Å; Figure 3); the angle between the bases equals 127.4(1)°. The shortest distance between the bases of one chain and the methyl groups of the next chain in direction of the y axis amounts to 3.455(7) Å (C13···C5 ($0.5-x$, $-0.5+y$, z)). In the direction of the z axis chains are linked by hydrogen bonds between (N1)H and the not methylated phosphonic acid oxygen O14 (2.844(4) Å, $0.5+x$, $0.5-y$, $1-z$).

Surprisingly, the solid-state structure of 6Umpapr shows distinct similarities to that of H_2(6Umpa) (Figure 4). The uracil bases of neighboring molecules are arranged in planar infinite layers connected by two different pairs of hydrogen bonds about centers of inversion (N3···O4 ($-x$, $1-y$, $-z$) 2.809(3) Å, N1···O2 ($1-x$, $2-y$, $-z$) 2.798(3) Å). As in H_2(6Umpa), (C5)H in 6Umpapr appears to be involved in a weak hydrogen bond (C5···O14 ($-1+x$, y, z) 3.264(3) Å);

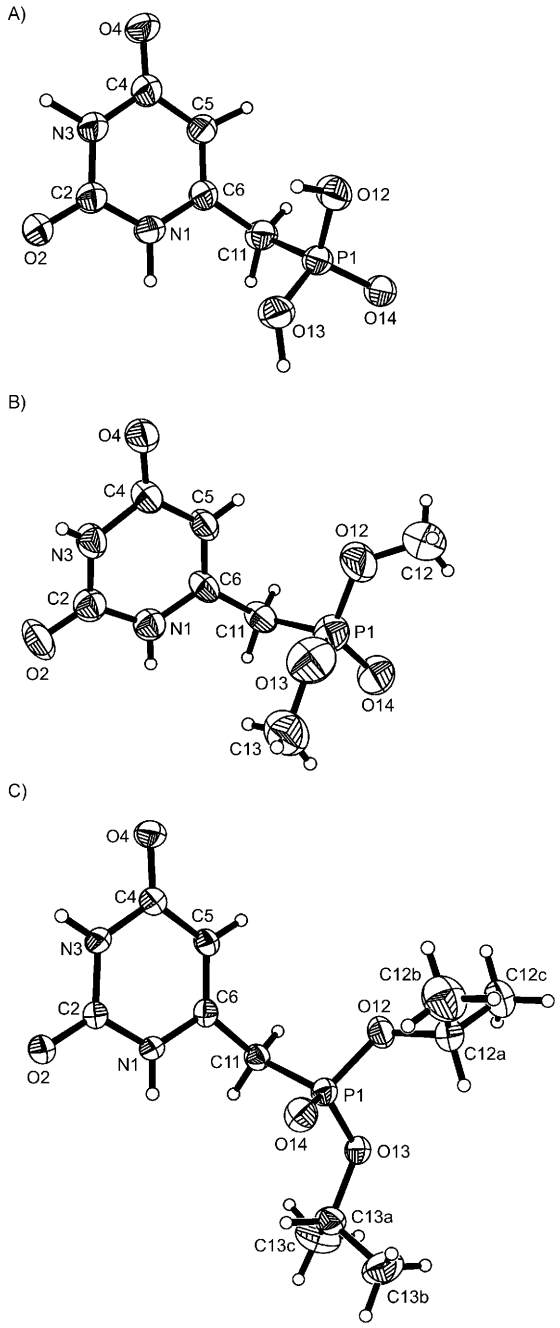

Figure 2. Molecular structure and atom numbering scheme of H_2(6Umpa) (A),[12] 6Umpame (B), and 6Umpapr (C). Displacement ellipsoids are drawn at the 50% probability level.

clearly, the distance of 3.264 Å is rather long, but the geometry is favorable.

Bifurcated hydrogen bonding between the uracil bases and two phosphonic acid oxygen atoms of a neighboring molecule as in H_2(6Umpa)[12] is not observed, probably due to steric reasons. Also no stacking interactions between the uracil bases are observed in either of the solid-state structures of these diesters. Though it is notable that the distances between the planes of the nucleobases are in the range of 3.4–3.5 Å, no substantial overlap between aromatic rings

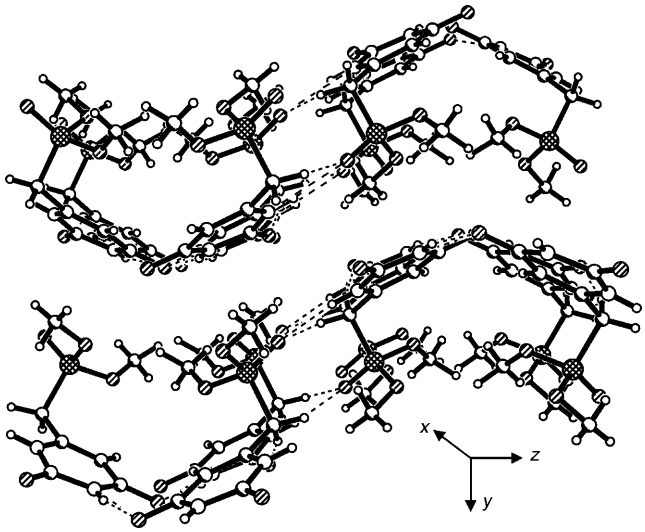

Figure 3. Section of the three-dimensional arrangement of 6Umpame molecules in the solid-state structure viewed along the crystallographic *x* axis. See Section 2.1 for details.

is observed and any overlap between a uracil base and a substituent of a neighboring base is small. These solid-state results indicate that both esters exist in solution as monomeric species with little or no intramolecular interactions, thus providing these neutral molecules with a high flexibility that should facilitate their passage through cell membranes.

2.2. Definition of equilibrium constants and preliminary results: A phosphonate group may accept two protons, thus leading to the $P(O)(OH)_2$ group, but the release of the first proton occurs with $pK_a < 2.5$, for example, $pK_{a/1} = 2.10 \pm 0.03$[13] for $CH_3P(O)(OH)_2$ or $pK_{a/1} = 1.71 \pm 0.10$ for $CH_3CH_2OCH_2CH_2P(O)(OH)_2$;[14] therefore, this reaction is not of relevance in the pH range above four used in this study. Herein, only the second deprotonation step needs to be considered together with the deprotonation reaction of the uracil residue[15,16] and this then gives rise to Equilibria (1) and (2), in which $Umpa^{2-}$ represents both $5Umpa^{2-}$ and $6Umpa^{2-}$:

$$H(Umpa)^- \rightleftharpoons Umpa^{2-} + H^+ \quad (1a)$$

$$K^H_{H(Umpa)} = \frac{[Umpa^{2-}][H^+]}{[H(Umpa)^-]} \quad (1b)$$

$$Umpa^{2-} \rightleftharpoons (Umpa-H)^{3-} + H^+ \quad (2a)$$

$$K^H_{Umpa} = \frac{[(Umpa-H)^{3-}][H^+]}{[Umpa^{2-}]} \quad (2b)$$

The corresponding acidity constants have recently been determined:[12] $pK^H_{H(5Umpa)} = 7.15 \pm 0.01$, $pK^H_{5Umpa} = 10.25 \pm 0.02$ and $pK^H_{H(6Umpa)} = 6.17 \pm 0.02$, $pK^H_{6Umpa} = 10.12 \pm 0.02$ (25 °C; $I = 0.1$ M, $NaNO_3$). The deprotonation of the uracil residue is expected to occur to the largest degree at (N3)H, but the

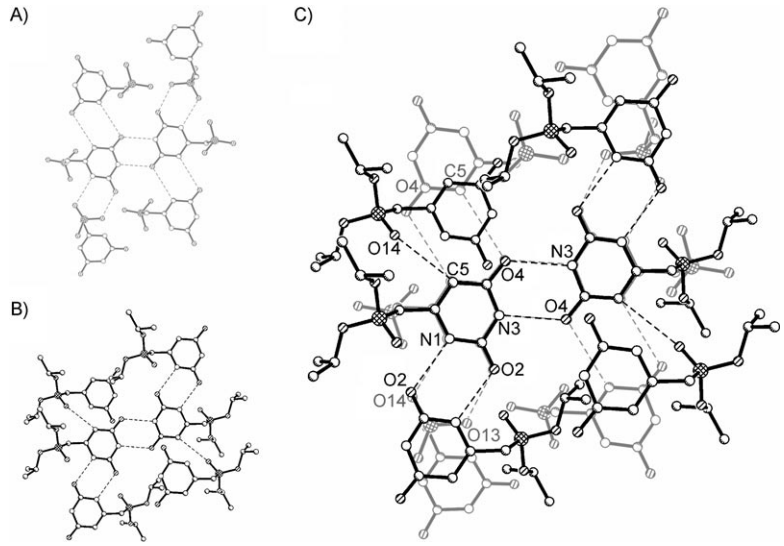

Figure 4. Section of hydrogen-bonded network in H_2(6Umpa) (A)[12] and 6Umpapr (B) as well as a superimposition of both structures with H_2(6Umpa) in gray to illustrate the similarities (C). Hydrogen atoms have been omitted for clarity. See Section 2.1 for details.

acidity of the (N1)H unit is also not expected to be much smaller. Regarding the tautomeric equilibrium for uracil itself, it was concluded that the (N3)-deprotonated species dominates at about 80 % in aqueous solution.[12] The conclusion that the (N3)H site is the more acidic one is also in accordance with a recent first principles quantum mechanics calculation.[17]

Complex formation with a monoprotonated phosph(on)ate group is very weak[18] and not of relevance here. Indeed, the experimental data of the potentiometric pH titrations of the metal-ion-containing systems can be fully described by considering the two acid–base equilibria defined above [Eqs. (1) and (2)], as well as the two complex forming equilibria given below [Eqs. (3) and (4)], provided that the evaluation of the data is restricted to the pH range before the onset of the formation of hydroxo complexes, which was evident from the titration of M^{2+} without ligand (see Section 4.2). Hence, initially the uncharged complex M(Umpa) forms [Eq. (3)], which may then lose a proton from the uracil residue [Eq. (4)] to give the anionic species $M(Umpa-H)^-$:

$$M^{2+}+Umpa^{2-} \rightleftharpoons M(Umpa) \quad (3a)$$

$$K^{M}_{M(Umpa)} = \frac{[M(Umpa)]}{[M^{2+}][Umpa^{2-}]} \quad (3b)$$

$$M(Umpa) \rightleftharpoons M(Umpa-H)^- + H^+ \quad (4a)$$

$$K^{H}_{M(Umpa)} = \frac{[M(Umpa-H)^-][H^+]}{[M(Umpa)]} \quad (4b)$$

The corresponding results, obtained from excellent fits of the fitting procedures, are listed in columns 3 and 6 of Table 1, respectively. It may be added that the previously determined values for the Mg^{2+} and Ca^{2+} complexes[19] are in perfect accordance with those reported herein. Further, the acidity constants [Eq. (4)] for the formation of $Cu(5Umpa-H)^-$ and $Zn(5Umpa-H)^-$ could not be measured due to hydrolysis of $Cu^{2+}_{(aq)}$ and $Zn^{2+}_{(aq)}$. In addition, the very low degree of formation of the Cu(6Umpa) complex prevented measurement of the stability constant with a reasonable error limit; in other words, once formed it lost a proton and transformed into the deprotonated $Cu(6Umpa-H)^-$ complex. Therefore, the formation of $Cu(6Umpa-H)^-$ was evaluated by keeping the calculated value (see below) for Cu(6Umpa) constant; this procedure is justified because none of the M(6Umpa) complexes showed an increased stability (Section 2.3) and this is also true for the measured, though error-prone, values (see above) for Cu(6Umpa).

Finally, it needs to be emphasized that the results listed in column 6 (and also in column 7) of Table 1 are apparent constants only because the formation of $M_2(Umpa-H)^+$ was ignored (see Section 2.4). In contrast, the stability constants for the M(Umpa) complexes are of a final nature and they show the usual trends: for the alkaline earth ions, complex stability decreases with increasing ionic radii, and for the divalent 3d metal ions, the long-standing experience[20] is confirmed that stabilities of phosph(on)ate–metal-ion complexes often do not strictly follow[11,18,21] the Irving–Williams series[22] because the Mn^{2+} complexes are especially stable.[11,18,21]

2.3. Evaluation of the stabilities of the M(Umpa) complexes: The following question needs to be answered for the M(5Umpa) and M(6Umpa) complexes: Are the stabilities of these species solely determined by the coordinating properties of the phosphonate group or does the uracil residue also have an effect? An answer may be found by making use of the earlier established straight-line correlations[21,23] for $\log K^{M}_{M(R-PO_3)}$ versus $pK^{H}_{H(R-PO_3)}$ plots, in which $R-PO_3^{2-}$ represents phosphate monoester[24] or phosphonate ligands,[25] of which R is unable to interact with metal ions. Four examples of such plots are shown in Figure 5 for the 1:1 complexes of Ca^{2+}, Zn^{2+}, Cd^{2+}, and Cu^{2+} with eight simple ligands allowing only a phosph(on)ate coordination (open circles). The solid points refer to the $5Umpa^{2-}$ and $6Umpa^{2-}$ complexes of the mentioned metal ions. Evidently the data points for all M(6Umpa) complexes fit on the cor-

Table 1. Logarithms of the stability constants of complexes of M(5Umpa) and M(6Umpa) [Eq. (3)] together with the negative logarithms of the acidity constants [Eq. (4)], which are apparent (app) constants in these cases (see Section 2.4), of the same M(Umpa) complexes as determined (exptl) by potentiometric pH titrations in aqueous solution. For comparison the calculated (calcd) stability constants of the M(Umpa) complexes [Eq. (5)] are also given, as well as the stability enhancements $\log \Delta_{M/U}$ [Eq. (6)] and the extent of the acidification of the uracil residue in the M(Umpa) complexes as defined by $\Delta pK_{a/M(Umpa)}$ [Eq. (11)]; again, these are apparent values (25 °C; $I = 0.1$ M, $NaNO_3$).[a]

U^{2-}	M^{2+}	$\log K^{M}_{M(Umpa)exptl}$	$\log K^{M}_{M(Umpa)calcd}$	$\log \Delta_{M/Umpa}$	$pK^{H}_{M(Umpa)app}$	$\Delta pK_{a/M(Umpa)app}$
$5Umpa^{2-}$	Mg^{2+}	1.79 ± 0.03[b]	1.76 ± 0.04	0.03 ± 0.05	9.44 ± 0.02[b]	0.81 ± 0.03
	Ca^{2+}	1.60 ± 0.03[b]	1.57 ± 0.05	0.03 ± 0.06	9.48 ± 0.03[b]	0.77 ± 0.04
	Mn^{2+}	2.52 ± 0.03	2.38 ± 0.05	0.14 ± 0.06	9.09 ± 0.07	1.16 ± 0.07
	Co^{2+}	2.26 ± 0.02	2.15 ± 0.06	0.11 ± 0.06	8.69 ± 0.08	1.56 ± 0.08
	Cu^{2+}	3.58 ± 0.04	3.31 ± 0.06	0.27 ± 0.07	–[c]	–
	Zn^{2+}	2.58 ± 0.02	2.45 ± 0.06	0.13 ± 0.06	–[c]	–
	Cd^{2+}	2.83 ± 0.03	2.75 ± 0.05	0.08 ± 0.06	8.42 ± 0.07	1.83 ± 0.07
$6Umpa^{2-}$	Mg^{2+}	1.50 ± 0.04[b]	1.56 ± 0.04	-0.06 ± 0.06	9.48 ± 0.04[b]	0.64 ± 0.04
	Ca^{2+}	1.40 ± 0.05[b]	1.44 ± 0.05	-0.04 ± 0.07	9.39 ± 0.03[b]	0.73 ± 0.04
	Mn^{2+}	2.10 ± 0.03	2.15 ± 0.05	-0.05 ± 0.06	8.51 ± 0.06	1.61 ± 0.06
	Co^{2+}	1.92 ± 0.06	1.93 ± 0.06	-0.01 ± 0.08	7.83 ± 0.04	2.29 ± 0.04
	Cu^{2+}	2.85[d]	2.85 ± 0.06	0	5.45 ± 0.03	4.67 ± 0.04
	Zn^{2+}	2.11 ± 0.10	2.11 ± 0.06	0.00 ± 0.12	6.35 ± 0.10	3.77 ± 0.10
	Cd^{2+}	2.41 ± 0.04	2.43 ± 0.05	-0.02 ± 0.06	7.01 ± 0.03	3.11 ± 0.04

[a] The error limits are three times the standard error of the mean value (3σ) or the sum of the probable systematic errors, whichever is larger. The error limits (3σ) of the derived data, here for columns 5 and 7 (and also in the text), were calculated according to the error propagation after Gauss. The acidity constants of $H(5Umpa)^-$ and $H(6Umpa)^-$ [Eqs. (1) and (2)] are $pK^{H}_{H(5Umpa)} = 7.15 \pm 0.01$, $pK^{H}_{5Umpa} = 10.25 \pm 0.02$, $pK^{H}_{H(6Umpa)} = 6.17 \pm 0.02$ and $pK^{H}_{6Umpa} = 10.12 \pm 0.02$.[12] [b] These values are in excellent agreement with an earlier determination.[19] [c] These acidity constants could not be measured due to hydrolysis of $M(aq)^{2+}$. [d] Due to the low degree of formation of the Cu(6Umpa) species this constant could not be measured with satisfying accuracy; therefore, the calculated value (from column 4) was kept constant in the other calculations.

responding reference lines, whereas for some of the M(5Umpa) species an enhanced stability is observed.

A quantitative evaluation of the situation seen in Figure 5 is possible: The parameters for the corresponding straight-line equations, that is, the slopes m and the intercepts b with the y axis, which are defined by Equation (5), were tabulated.[21,23,25,26]

$$\log K^{M}_{M(R-PO_3)} = m\, pK^{H}_{H(R-PO_3)} + b \quad (5)$$

Hence, with a known pK_a value for the deprotonation of a $P(O)_2(OH)^-$ group, an expected stability constant can be calculated for any phosph(on)ate–M^{2+} complex. Indeed, application of $pK^{H}_{H(5Umpa)} = 7.15$ and $pK^{H}_{H(6Umpa)} = 6.17$ to Equation (5) provides the calculated stability constants, $K^{M}_{M(Umpa)calcd}$, which are listed in column 4 of Table 1.

Stability enhancements, such as those seen in Figure 5, can be quantified by the differences between experimentally (exptl) measured stability constants and those calculated (calcd) according to Equation (5); this is defined by Equation (6) and values are listed in Table 1, column 5.

$$\log \Delta_{M/Umpa} = \log K^{M}_{M(Umpa)exptl} - \log K^{M}_{M(Umpa)calcd} \quad (6a)$$

$$= \log K^{M}_{M(Umpa)} - \log K^{M}_{M(Umpa)op} \quad (= \log \Delta) \quad (6b)$$

Clearly, the expressions $\log K^{M}_{M(Umpa)calcd}$ and $\log K^{M}_{M(Umpa)op}$ are synonymous because the calculated value equals the stability constant of the so-called "open" (op) isomer, $M(Umpa)_{op}$ (see below), in which only a PO_3^{2-}/M^{2+} interaction occurs.

The $\log \Delta_{M/6Umpa}$ values for all M(6Umpa) systems are zero within the error limits (Table 1, column 5) and this means that in all these complexes only a PO_3^{2-}/M^{2+} interaction occurs. This is in contrast to the M(5Umpa) complexes in which a small but significant stability enhancement is observed in several instances, that is, $\log \Delta_{M/5Umpa} > 0$. This result must mean[21,27] that even though the phosphonate group is the primary binding site, a further interaction of the phosphonate-coordinated metal ion must occur; in other words, any stability enhancement according to Equation (6) reflects an additional interaction.[27] The structure of $5Umpa^{2-}$ in Figure 1 immediately reveals that the only additional binding site that the phosphonate-coordinated M^{2+} can reach is the carbonyl oxygen at C4, thus giving rise to the formation of a seven-membered chelate. Already from the varying stability enhancements in Table 1 (column 5) it follows that this additional interaction varies from metal ion to metal ion. Hence, we have to consider an isomeric equilibrium between an open (op) and a closed (cl) or chelated form:

$$M(5Umpa)_{op} \rightleftharpoons M(5Umpa)_{cl} \quad (7)$$

The position of Equilibrium (7) is defined by the intramolecular and dimensionless constant K_I [Eq. (8)]:

$$K_I = \frac{[M(5Umpa)_{cl}]}{[M(5Umpa)_{op}]} \quad (8)$$

The interrelation between K_I and the stability enhancement $\log \Delta_{M/5Umpa}$ is given by Equation (9) as reported previously:[18,21,23,27]

$$K_I = \frac{K^{M}_{M(5Umpa)}}{K^{M}_{M(5Umpa)op}} - 1 = 10^{\log \Delta} - 1 \quad (9)$$

The percentage of the closed or chelated isomer in Equilibrium (7) follows from Equation (10):

$$\% M(5Umpa)_{cl} = \frac{100 K_I}{1 + K_I} \quad (10)$$

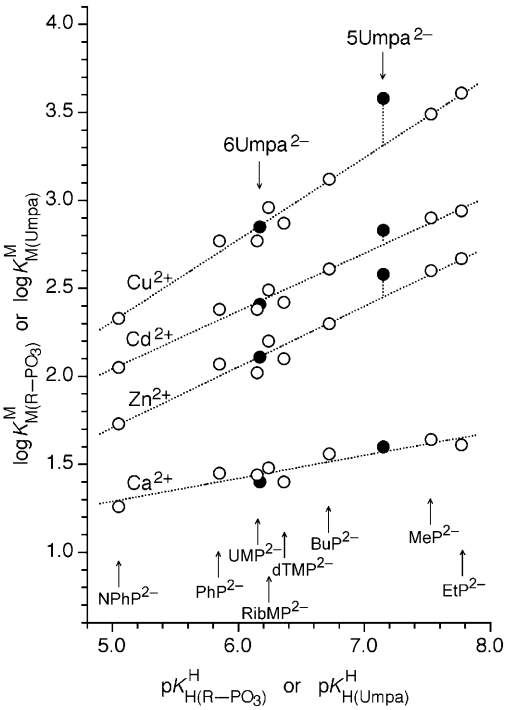

Figure 5. Evidence for an enhanced stability of several M(5Umpa) complexes and for the lack of such an enhanced stability of the M(6Umpa) species (●) based on the relationship between $\log K^{M}_{M(R-PO_3)}$ and $pK^{H}_{H(R-PO_3)}$ for M(R–PO_3) complexes of some simple phosphate monoester and phosphonate ligands (R–PO_3^{2-}) (○): 4-nitrophenyl phosphate ($NPhP^{2-}$), phenyl phosphate (PhP^{2-}), uridine 5′-monophosphate (UMP^{2-}), D-ribose 5-monophosphate ($RibMP^{2-}$), thymidine (=1-(2′-deoxy-β-D-ribofuranosyl)thymine) 5′-monophosphate ($dTMP^{2-}$), *n*-butyl phosphate (BuP^{2-}), methanephosphonate (MeP^{2-}), and ethanephosphonate (EtP^{2-}) (from left to right). The least-squares lines [Eq. (5)] are drawn through the corresponding eight data sets (○) taken from ref. [24] for the phosphate monoesters and from ref. [25] for the phosphonates. The points due to the equilibrium constants for the M^{2+}/$Umpa^{2-}$ systems (●) are based on the values listed in Table 1. The vertical broken lines emphasize the stability differences from the reference lines; they equal $\log \Delta_{M/Umpa}$, as defined in Equation (6), for the M/Umpa complexes. All the plotted equilibrium constants refer to aqueous solutions at 25 °C and $I = 0.1$ M ($NaNO_3$).

Application of this procedure yields the results listed in Table 2: The extent of chelate formation varies between about zero (or traces) for the alkaline earth ions and about 45 % for Cu^{2+}. For the other M(5Umpa) complexes the percentages of the chelates vary between about 15 and 30 %. Simplified structures of the open and the closed species of the M(5Umpa) complexes [Eq. (7)] are shown, together with the structure of the M(6Umpa) species, in the left part of Figure 6.

2.4. Considerations on M^{2+}–Umpa 1:1 complexes with deprotonated uracil residues and formation of $M_2(Umpa-H)^+$ species: In Section 2.2 we have already seen that the M(Umpa) complexes may lose a proton, thus giving rise to Equilibrium (4a). The corresponding acidity constants, $pK^{H}_{M(Umpa)}$, are listed in column 6 of Table 1. Since metal ion coordination at the phosphonate group neutralizes the negative charge at the side chain, one expects that uracil deprotonation is facilitated compared with the situation in free $Umpa^{2-}$ and the extent of this acidification can be quantified by Equation (11):

Table 2. Extent of chelate formation in M(5Umpa) complexes [Eq. (7)][a] as calculated from the stability enhancement $\log \Delta_{M/5Umpa}$ [Eq. (6)] and quantified by the dimensionless equilibrium constant K_I [Eqs. (8) and (9)] and the percentage of the chelated isomers $M(5Umpa)_{cl}$ [Eq. (10)] in aqueous solution (25 °C; $I = 0.1$ M, $NaNO_3$).[b]

M^{2+}	$\log \Delta_{M/5Umpa}$[c]	K_I	% $M(5Umpa)_{cl}$
Mg^{2+}	0.03 ± 0.05	0.07 ± 0.12	0 (7 ± 11)
Ca^{2+}	0.03 ± 0.06	0.07 ± 0.15	0 (7 ± 12)
Mn^{2+}	0.14 ± 0.06	0.38 ± 0.19	28 ± 10
Co^{2+}	0.11 ± 0.06	0.29 ± 0.18	22 ± 11
Cu^{2+}	0.27 ± 0.07	0.86 ± 0.30	46 ± 9
Zn^{2+}	0.13 ± 0.06	0.35 ± 0.19	26 ± 10
Cd^{2+}	0.08 ± 0.06	0.20 ± 0.17	17 ± 11

[a] The extent of chelate formation for the M(6Umpa) complexes is zero within the error limits because there is no stability enhancement observed for these species, that is, $\log \Delta_{M/6Umpa}$ is zero within the error limits (see Table 1, column 5). [b] For the error limits see footnote [a] of Table 1. [c] These values are from the upper part of column 5 in Table 1.

$$\Delta pK_{a/M(Umpa)} = pK^{H}_{Umpa} - pK^{H}_{M(Umpa)} \quad (11)$$

Indeed, that such an acidification occurs is evident from column 7 in Table 1. Furthermore, that in the chelated $M(5Umpa)_{cl}$ species the deprotonation of (N3)H is further facilitated by the interaction of M^{2+} with (C4)O (structure in the upper part of Figure 6) is quite plausible. The very strong acidification observed for the M(6Umpa) complexes containing a 3d metal ion is more of a surprise. Clearly, this can only mean that in these species (N1)H is deprotonated (note, (N1)H is only somewhat less acidic than (N3)H; Section 2.2) and that then six-membered chelates form; a simplified structure of $M(6Umpa-H)^-_{cl}$ is shown in the lower part of Figure 6.

The given interpretation for the $M(5Umpa-H)^-$ and $M(6Umpa-H)^-$ species appears to be quite straightforward, yet there are two caveats here: 1) The extent of an acidification of more than four p*K* units (Table 1, column 7) as observed for Cu(6Umpa) appears to be very large. 2) Because the experiments were carried out with an excess of metal ions, relative to the Umpa concentration, one could speculate that the $M(Umpa-H)^-$ species formed in Equilibrium (4a) would bind a second metal ion according to Reaction (12) and that this would further facilitate the deprotonation reaction of the uracil residue.

$$M(Umpa-H)^- + M^{2+} \rightleftharpoons M_2(Umpa-H)^+ \quad (12a)$$

$$K^{M(Umpa-H)}_{M_2(Umpa-H)} = \frac{[M_2(Umpa-H)^+]}{[M(Umpa-H)^-][M^{2+}]} \quad (12b)$$

Indeed, in some experiments a slight dependence of $pK^{H}_{M(Umpa)}$ on the M^{2+} concentration used could be observed, although it was never dramatic and always within the error limits (Table 1, column 6).

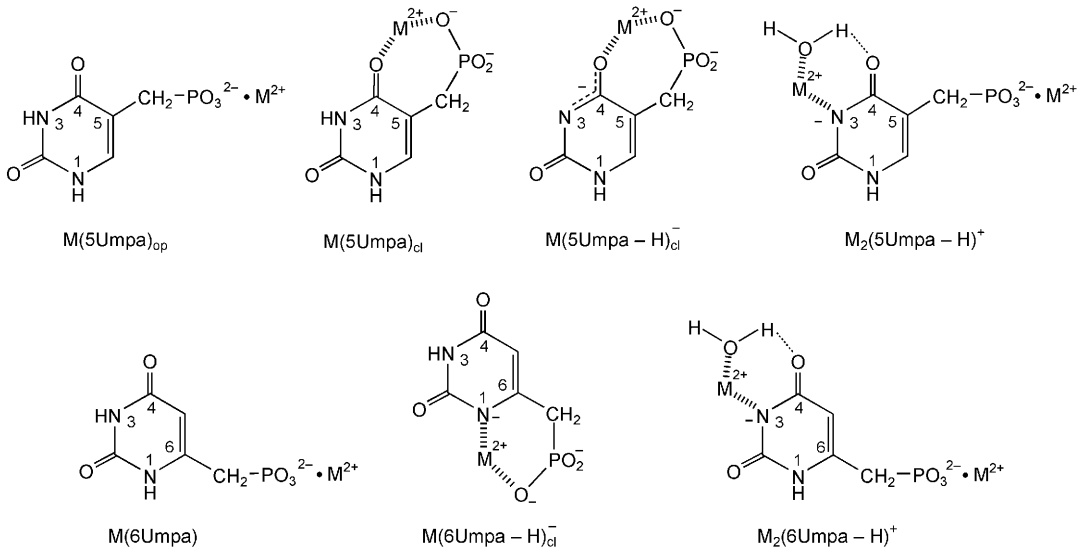

Figure 6. Metal-ion-binding modes in the various complexes formed with $5Umpa^{2-}$ (upper part) or $6Umpa^{2-}$ (lower part). In the complexes formed with $(Umpa-H)^{3-}$ species and where the negative charge is shown on N it can be delocalized in part to the neighboring C(O) group. For a discussion of the structures see text.

Our attempts to fit the experimental data with a model that also contained the $M_2(Umpa-H)^+$ species were not successful. No constants for the $M_2(Umpa-H)^+$ species were obtained and the already excellent fits were not improved any further. Considering the fact that the formation of the $M_2(Umpa-H)^+$ species is only a follow-up of the deprotonation Reaction (4) this is not surprising. Therefore, we took a different approach to the problem by employing the straight-line plots of $\log K^{M}_{M(Ur-H)}$ versus pK^{H}_{Ur} [in analogy to Eq. (5)], which had been recently determined for a series of uridinate derivatives (Ur).[28] In other words, with a known pK_a value for the deprotonation of (N3)H, the metal ion affinity of this site can be calculated. Since a metal ion coordinated to the phosphonate residue gives rise to an uncharged side chain, we concluded that the pK_a values of (N3)H in the open forms of M(5Umpa) and M(6Umpa) are well represented by the pK_a values of 5-methyluracil ($pK^{H}_{5MeUr}=9.82$)[12] and 6-methyluracil ($pK^{H}_{6MeUr}=9.55$).[12] These acidity constants were used together with the straight-line parameters[28] to calculate stability constants corresponding to Equilibrium (12a) for the formation of the $M_2(Umpa-H)^+$ complexes. It should be emphasized that, in case the pK_a values used should vary by 0.2 pK units, this has only a minor effect on the calculated stability constants because the slopes, m, of the straight lines [see also Eq. (5)] only vary between about 0.1 and 0.4. In the case of Cu^{2+} the slope ($m=0.457$) of the straight line is based on only two points,[28] and therefore, the very large error limit[28] of 0.21 log units was used and also taken into account in the calculation for $pK^{H}_{Cu(6Umpa)}$. To conclude, the stability constants for the $M_2(Umpa-H)^+$ complexes [Eq. (12)] (see Table 3, column 4) were kept constant in the fitting procedure and values for $pK^{H}_{M(Umpa)}$ [Eq. (4)] were newly calculated; the stability constants of the M(Umpa) complexes [Eq. (3)] remained unchanged. The fit was excellent in all instances and the results are summarized in Table 3.

We are convinced that the $pK^{H}_{M(Umpa)}$ values listed in Table 3 (column 5) are chemically more correct and that the corresponding data given in Table 1 (column 6) are only apparent constants. The $\Delta pK_{a/M(Umpa)}$ values [Eq. (6)] listed in column 6 of Table 3 are, as expected, somewhat smaller than those given in Table 1. Clearly, the size of these $\Delta pK_{a/M(Umpa)}$ values still depends strongly on the M^{2+} considered and this shows that the extent of chelate formation in the systems must vary (see below). However, the fact that $pK^{H}_{Mg(6Umpa)}=9.54\pm0.03$ and $pK^{H}_{Ca(6Umpa)}=9.49\pm0.04$ (Table 3) are identical within the error limits with $pK^{H}_{6MeUr}=9.55\pm0.05$[12] confirms the validity of the above assumptions; note, with $Mg(6Umpa-H)^-$ and $Ca(6Umpa-H)^-$ only charge neutralization is in effect and no chelate formation occurs (see also Section 2.5).

2.5. Extent of chelate formation in the M(Umpa−H)$^-$ complexes: If one considers, for example, the acidification due to the formation of the $M(5Umpa-H)^-$ complexes of the alkaline earth ions, which amounts to $\Delta pK_{a/M(5Umpa)}\approx0.70$ with the corresponding value of $\Delta pK_{a/Co(5Umpa)}\approx1.5$ for the $Co(5Umpa-H)^-$ complex (Table 3; upper part), it is evident that the "intensity" of the M^{2+} interaction with (C4)O varies reflecting different degrees of formation of the (N3)H-deprotonated chelates. The corresponding observations are made with the $M(6Umpa-H)^-$ complexes. Hence, the question arises, what is the position of the intramolecular Equilibrium (13a)?

$$M(Umpa-H)^-_{op} \rightleftharpoons M(Umpa-H)^-_{cl} \qquad (13a)$$

$$K_I^* = \frac{[M(Umpa-H)_{cl}^-]}{[M(Umpa-H)_{op}^-]} \quad (13b)$$

Table 3. Reevaluation of the experimental data of the potentiometric pH titrations by taking into account the estimated stabilities of the $M_2(Umpa-H)^+$ species [Eq. (12)], leading to the logarithms of the stability constants of M(Umpa) complexes [Eq. (3)] and the negative logarithms of the acidity constants of the M(Umpa) species [Eq. (4)], from which the extent of the acidification of the uracil residue in the M(Umpa) complexes follows, as defined by $\Delta pK_{a/M(Umpa)}$ [Eq. (11)] (25 °C; $I = 0.1$ M, $NaNO_3$).[a]

U^{2-}	M^{2+}	$\log K^{M}_{M(Umpa)}$ [b]	$\log K^{M(Umpa)}_{M_2(Umpa)calcd}$ [c]	$pK^{H}_{M(Umpa)}$	$\Delta pK_{a/M(Umpa)}$
$5Umpa^{2-}$	Mg^{2+}	1.79 ± 0.03	0.82 ± 0.05	9.52 ± 0.02	0.73 ± 0.03
	Ca^{2+}	1.60 ± 0.03	0.91 ± 0.04	9.58 ± 0.02	0.67 ± 0.03
	Mn^{2+}	2.52 ± 0.03	1.44 ± 0.05	9.13 ± 0.06	1.12 ± 0.06
	Co^{2+}	2.26 ± 0.02	1.78 ± 0.05	8.79 ± 0.06	1.46 ± 0.06
	Cu^{2+}	3.58 ± 0.04	4.43 ± 0.21 [d]	– [e]	–
	Zn^{2+}	2.58 ± 0.02	2.68 ± 0.07	– [e]	–
	Cd^{2+}	2.83 ± 0.03	3.46 ± 0.05	9.12 ± 0.15 [f]	1.13 ± 0.15
$6Umpa^{2-}$	Mg^{2+}	1.50 ± 0.04	0.79 ± 0.05	9.54 ± 0.03	0.58 ± 0.04
	Ca^{2+}	1.40 ± 0.05	0.87 ± 0.04	9.49 ± 0.04	0.63 ± 0.04
	Mn^{2+}	2.10 ± 0.03	1.39 ± 0.05	8.58 ± 0.03	1.54 ± 0.04
	Co^{2+}	1.92 ± 0.06	1.69 ± 0.05	7.90 ± 0.04	2.22 ± 0.04
	Cu^{2+}	2.85	4.30 ± 0.21 [d]	6.49 ± 0.27 [g]	3.63 ± 0.27
	Zn^{2+}	2.11 ± 0.10	2.56 ± 0.07	6.52 ± 0.07	3.60 ± 0.07
	Cd^{2+}	2.41 ± 0.04	3.35 ± 0.05	7.68 ± 0.05	2.44 ± 0.05

[a] For the error limits see footnote [a] of Table 1. [b] These values remained unchanged and are identical to those listed in column 3 of Table 1. [c] These values were calculated with the published[28] straight-line parameters (see Section 2.4) and the acidity constants[12] of 5-methyluracil (5MeUr = thymine), $pK^{H}_{5MeUr} = 9.82$ (upper part of the table), and 6-methyluracil (6MeUr), $pK^{H}_{6MeUr} = 9.55$ (lower part). [d] This error limit is a deliberately large estimate because the straight line in this case is only based on two data points.[28] [e] These acidity constants could not be measured due to hydrolysis of $M(aq)^{2+}$. [f] The degree of formation of $Cd(5Umpa-H)^-$ in the experiments was rather low, and therefore, the error limit was increased from 0.09 (3σ) to 0.15 to be on the safe side. [g] This error limit is large because of the large error limit of 4.30 ± 0.21 (column 4).

Therefore, an interrelation between the extent of the acidification and K_I^* needs to be developed. There are various ways to achieve this and a convenient procedure for the present case is outlined below.[29] Since $\log K^{M}_{M(Umpa\text{-}H)}$ is connected with $pK^{H}_{M(Umpa)}$ [Eq. (4)] through Equation (14), the stability enhancement, commonly expressed as $\log \Delta$ [cf. Eq. (6)], can also be defined by Equation (15), in which the first term on the right-hand side is the acidity constant of the open isomer [Eq. (16)], whereas the second one is the experimentally measured constant as defined by Equilibrium (4a) and Equation (4b).

$$\log K^{M}_{M(Umpa\text{-}H)} = \log K^{M}_{M(Umpa)} + pK^{H}_{Umpa} - pK^{H}_{M(Umpa)} \quad (14)$$

$$\log \Delta^*_{M/(Umpa\text{-}H)} = pK^{H}_{M(Umpa)op} - pK^{H}_{M(Umpa)} \quad (= \log \Delta^*) \quad (15)$$

$$K^{H}_{M(Umpa)op} = \frac{[M(Umpa-H)_{op}^-][H^+]}{[M(Umpa)]} \quad (16)$$

Clearly, by considering Equilibrium (13a), Equation (4b) can be rewritten to give Equation (17a) and by taking into account Equation (13b) one obtains Equation (17d):

$$K^{H}_{M(Umpa)} = \frac{([M(Umpa-H)_{op}^-] + [M(Umpa-H)_{cl}^-])[H^+]}{[M(Umpa)]} \quad (17a)$$

$$= K^{H}_{M(Umpa)op} + K^{H}_{M(5Umpa)cl} \quad (17b)$$

$$= K^{H}_{M(Umpa)op} + K_I^* K^{H}_{M(Umpa)op} \quad (17c)$$

$$= K^{H}_{M(5Umpa)op}(1 + K_I^*) \quad (17d)$$

Equation (18a) follows from Equation (17d), and by including Equation (15) Equation (18b) can be obtained:

$$K_I^* = \frac{K^{H}_{M(Umpa)}}{K^{H}_{M(Umpa)op}} - 1 \quad (18a)$$

$$= 10^{\log \Delta^*} - 1 \quad (18b)$$

Now that K_I^* is known, the percentage of the closed isomer, $M(Umpa-H)_{cl}^-$, can be calculated in an analogous manner to Equation (10).

To be able to apply Equations (15) and (18b), an acidity constant for the open isomer, $M(Umpa)_{op}$, needs to be estimated. Again we use the argument already put forward in Section 2.4, that is, $pK^{H}_{M(5Umpa)op}$ and $pK^{H}_{M(6Umpa)op}$ are well represented by $pK^{H}_{5MeUr} = 9.82$ and $pK^{H}_{6MeUr} = 9.55$, respectively, because in all instances the proton at the uracil residue is removed from a neutral species. To be on the safe side, we enlarge the error limits[12] from 0.05 to 0.15 in the application of $K^{H}_{H(Umpa)op}$ (Table 4, column 3). We employ the given estimation, being well aware that in the case of the formation of $M(6Umpa-H)_{cl}^-$ the proton needs to be removed from the (N1)H site (and not from the (N3)H unit as is more common),[12] although removal from (N3)H is also compatible, and actually quite likely, for $M(6Umpa-H)_{op}^-$ and is also required for $M_2(6Umpa-H)^+$ (see Figure 6). However, most importantly, the result obtained for the alkali earth ion complexes, that is, $\log \Delta^*_{M/(6Umpa\text{-}H)} \approx 0$ (Table 4, column 5), indicating a very low degree of formation, or even one of zero, for the $Mg(6Umpa-H)_{cl}^-$ and $Ca(6Umpa-H)_{cl}^-$ species, confirms the validity of the assumptions made because the affinity of Mg^{2+} and Ca^{2+} towards nitrogen sites is expected[28] to be small (see below).

The results based on Equations (15) and (18b) are assembled in Table 4 and they reveal several interesting points, a few of which are mentioned below:

1) For Mn^{2+}, Co^{2+}, and Cd^{2+}, the stability enhancements and thus the degrees of formation of the seven-membered chelates $M(5Umpa-H)_{cl}^-$ are smaller than those for the corresponding six-membered $M(6Umpa-H)_{cl}^-$ species; a behavior that is to be expected (and is also in accordance if $(N)^-$ versus (C)O affinities are compared).[30]

Table 4. Extent of intramolecular chelate formation [Eq. (13)] in several M(Umpa−H)$^-$ complexes of (5Umpa−H)$^{3-}$ and (6Umpa−H)$^{3-}$ as expressed by the dimensionless equilibrium constant K_I^* [Eqs. (13b) and (18)] and the percentage of the chelated isomers M(Umpa−H)$^-$ [analogous to Eq. (10)] in aqueous solution (25 °C; I = 0.1 M, $NaNO_3$).[a]

U^{2-}	M^{2+}	$pK^H_{M(Umpa)op}$ [b]	$pK^H_{M(Umpa)}$ [c]	$\log \Delta^*_{M/(U-H)}$	K_I^*	%M(U−H)$^-_{cl}$
5Umpa^{2-}	Mg^{2+}	9.82 ± 0.15	9.52 ± 0.02	0.30 ± 0.15	1.00 ± 0.70	50 ± 17
	Ca^{2+}	9.82 ± 0.15	9.58 ± 0.02	0.24 ± 0.15	0.74 ± 0.61	43 ± 20
	Mn^{2+}	9.82 ± 0.15	9.13 ± 0.06	0.69 ± 0.16	3.90 ± 1.82	80 ± 8
	Co^{2+}	9.82 ± 0.15	8.79 ± 0.06	1.03 ± 0.16	9.72 ± 3.99	91 ± 4
	Cd^{2+}	9.82 ± 0.15	9.12 ± 0.15	0.70 ± 0.21	4.01 ± 2.45	80 ± 10
6Umpa^{2-}	Mg^{2+}	9.55 ± 0.15	9.54 ± 0.03	0.01 ± 0.15	≈0	≈0
	Ca^{2+}	9.55 ± 0.15	9.49 ± 0.04	0.06 ± 0.16	≈0	≈0
	Mn^{2+}	9.55 ± 0.15	8.58 ± 0.03	0.97 ± 0.15	8.33 ± 3.29	89 ± 4
	Co^{2+}	9.55 ± 0.15	7.90 ± 0.04	1.65 ± 0.16	43.67 ± 15.97	98 ± 1
	Cu^{2+}	9.55 ± 0.15	6.49 ± 0.27	3.06 ± 0.31	1147 ± 817	99.9 ± 0.1
	Zn^{2+}	9.55 ± 0.15	6.52 ± 0.07	3.03 ± 0.17	1071 ± 408	99.9 ± 0.1
	Cd^{2+}	9.55 ± 0.15	7.68 ± 0.05	1.87 ± 0.16	73.13 ± 26.99	98.7 ± 0.5

[a] For the error limits see footnote [a] of Table 1. The calculations in this table are based on Equations (13) to (18). No values are available for Cu(5Umpa−H)$^-$ and Zn(5Umpa−H)$^-$ because of hydrolysis of the M(aq)$^{2+}$ species (see also Table 1 and Table 3). [b] It is assumed (see also text in Sections 2.4 and 2.5) that the acidity constant of 5MeUr represents that of M(5Umpa)$_{op}$ well, that is, $pK^H_{M(5Umpa)op} \approx pK^H_{5MeUr} = 9.82 \pm 0.05$; analogously it is assumed that $pK^H_{M(6Umpa)op} \approx pK^H_{6MeUr} = 9.55 \pm 0.05$.[12] To be on the safe side the error limits are increased from ± 0.05 to ± 0.15 in both instances and these values are listed above. [c] These values are from column 5 in Table 3.

1) It is evident that the phosphonate group is the binding site that determines the stability of the M(Umpa) complexes to the largest degree (Figure 5) as expected.
2) It is more of a surprise that the carbonyl group (C4)O has a significant affinity towards all metal ions studied, thus giving rise to the formation of seven-membered M(5Umpa)$_{cl}$ and M(5Umpa−H)$^-_{cl}$ chelates (Figure 6, upper part) and deserves to be noted because corresponding interactions are expected in nucleic acids if a metal ion is correctly positioned.
3) Furthermore, such a carbonyl/M^{2+} interaction facilitates deprotonation of the neighboring (N3)H group, which in turn then leads to higher degrees of formation of the chelated species, that is, M(5Umpa−H)$^-_{cl}$ versus M(5Umpa)$_{cl}$ (cf. Tables 2 and 4 and the structures in Figure 6, upper part).
4) The amide-type[30] complex formation that results from 3d ions including Zn^{2+} and Cd^{2+} in the M(6Umpa−H)$^-_{cl}$ species (Figure 6, lower part) is highly significant because deprotonation of the NH group occurs in the physiological pH range at around 7.5 (partly even below this value).
5) Of special interest is the formation of the M_2(Umpa−H)$^+$ complexes because this demonstrates that under certain conditions in a nucleotide one metal ion may bind to the phosphate group and another one to the nucleobase residue.

2) Most interesting, however, especially in the context of the previous point, is the fact that degrees of formation for Mg^{2+} and Ca^{2+} of about 50% are observed for the M(5Umpa−H)$^-_{cl}$ species despite the unfavorable chelate-ring size, whereas for the corresponding M(6Umpa−H)$^-_{cl}$ species the degree of formation is zero within the error limits. This confirms the well-known fact that Mg^{2+} and Ca^{2+} have a significant affinity towards carbonyl oxygen atoms[13,31,32] and only a very small one towards nitrogen (including N$^-$) sites.[28,31]
3) Comparison of the degrees of formation of the M(5Umpa)$_{cl}$ (Table 2) and M(5Umpa−H)$^-_{cl}$ species (Table 4) confirms the expectation that deprotonation of (N3)H leads to some delocalization of negative charge towards (C4)O and thus to an increased degree of formation of the M(5Umpa−H)$^-_{cl}$ isomers.
4) Also interesting is the very large degree of formation of the M(6Umpa−H)$^-_{cl}$ species of the 3d metal ions, including Zn^{2+} and Cd^{2+}, but this is in accordance with the properties of amide-type[30] binding sites.
5) Of further interest in this context is the hydrogen bond previously described[12] between (N1)H and the phosphonate group of 6Umpa^{2-} (see Section 2.1 and the structure in Figure 2A) because replacing the hydrogen with M^{2+} gives the corresponding chelate seen for M(6Umpa−H)$^-_{cl}$ in Figure 6 (lower part).

3. Conclusions

What have we learned from studying the coordination chemistry of 5Umpa^{2-} and 6Umpa^{2-}? Several insights, some of them trivial, others more surprising, have been obtained:

The structures of the M_2(Umpa−H)$^+$ species mentioned last deserve special comments as far as the nucleobase binding site is concerned because these are expected to depend on the kind of metal ion involved. For example, for Co^{2+} (and Ni^{2+}) it has been concluded[28] that in uridinate-type complexes, Co(Ur−H)$^+$, the metal ion is only coordinated in a monodentate fashion to (N3)$^-$, but for all other metal ions (considered herein) chelate formation must be surmised. Solid-state studies[33] of complexes containing a cytidine residue and Cd^{2+}, Zn^{2+}, or Cu^{2+} show that distorted 4-membered chelates form (see ref.[31] and references therein) by coordinating N3 and (C4)O; corresponding structures are expected[28] for uridinates and consequently also for the M_2(Umpa−H)$^+$ species. However, in aqueous solution it is highly likely that in addition to the four-membered rings, so-called semichelates form in which M^{2+} is innersphere bound to (N3)$^-$ and an M^{2+}-coordinated water interacts with

(C4)O, thus giving rise to an outersphere interaction (see the two structures to the right of Figure 6). Of course, a structure with two semichelates involving both (C2)O and (C4)O in an outersphere manner could also form, especially with larger cations, such as Cd^{2+}.

For $Mn_2(Umpa-H)^+$ one may propose the same structures as discussed above for Cd^{2+}, Zn^{2+}, or Cu^{2+} complexes. However, there is also a crystal structure in which Mn^{2+} coordinates to (C2)O of a cytidine residue with a rather short bond (2.08 Å).[33,34] Considering the partial delocalization of the negative charge from $(N3)^-$ to (C2)O and (C4)O, a semichelate involving, for example, an innersphere (C4)O and an outersphere $(N3)^-$ may well exist in aqueous solution in equilibrium. The same kind of semichelate is expected to occur with the alkaline earth ions; indeed, Ca^{2+} is known[35] to coordinate innersphere to (C4)O of a uridine residue in an RNA tetraplex. To conclude, M^{2+} binding to the deprotonated uracil residue in $M_2(Umpa-H)^+$ species may occur in different ways, and hence, isomeric equilibria are expected to exist in solution.

4. Experimental Section

4.1. Materials and equipment: 5- and 6-Uracilmethylphosphonic acid were synthesized as described[36] and used recently.[12,19] The methyl diester of 6Umpa (6Umpame) used in X-ray analysis was also prepared as described in reference [36] and 6Umpapr was synthesized as described in Section 4.3.

The disodium salt of 1,2-diaminoethane *N*,*N*,*N*′,*N*′-tetraacetic acid (Na_2H_2EDTA) and the nitrate salts of all divalent metal ions (all pro analysi) were obtained from Merck (Darmstadt, Germany). The exact concentrations of the stock solutions of the divalent metal ions were determined by potentiometric pH titrations through their EDTA complexes by measuring the equivalents of protons liberated from $H(EDTA)^{3-}$ upon complex formation. All the other reagents were the same as those used previously.[12]

The potentiometric pH titrations were carried out with the equipment described in the literature[12] and also the same buffer solutions were used for calibration of the instrument (for details see ref. [37]). Always a pair of solutions, that is, with and without ligand (also see below), were titrated and evaluated. All equilibrium constants were calculated by curve-fitting procedures by using a Newton–Gauss nonlinear least-squares program, as described previously.[38]

4.2. Determination of the stability and acidity constants of the M(Umpa) complexes: The conditions for the determination of the stability and acidity constants, $K^{M}_{M(Umpa)}$ [Eq. (3)] and $K^{H}_{M(Umpa)}$ [Eq. (4)], were the same as described[12] for the acidity constants [Eqs. (1) and (2)] of the ligands $H(5Umpa)^-$ and $H(6Umpa)^-$. This means aqueous 0.54 mM HNO_3 (50 mL, 25 °C, I = 0.1 M, $NaNO_3$) was titrated under N_2 in the presence and absence of approximately 0.3 mM $5Umpa^{2-}$ or $6Umpa^{2-}$ (obtained by adjusting the stock solutions of the $H_2(Umpa)$ acids to pH 8.5) with 0.03 M NaOH (1.5 mL). The exact Umpa concentration was calculated from the difference of the NaOH consumption between the two indicated titrations. In the titrations for the stability constants, $NaNO_3$ was partly or fully replaced by $M(NO_3)_2$ (M^{2+} = Mg^{2+}, Ca^{2+}, Mn^{2+}, Co^{2+}, Cu^{2+}, Zn^{2+}, or Cd^{2+}) by keeping I at 0.1 M. The M^{2+}/ligand ratios were about as follows: for 5Umpa, Mg^{2+} and Ca^{2+} (111:1, 89:1), Mn^{2+} and Zn^{2+} (14:1, 7:1), Co^{2+} (21:1, 14:1), Cu^{2+} (3:1, 1.5:1), and Cd^{2+} (7:1, 3.5:1); for 6Umpa, Mg^{2+} and Ca^{2+} (111:1, 89:1), Mn^{2+} (56:1, 28:1, 14:1), Co^{2+} (21:1, 14:1, 7:1), Cu^{2+} (4:1, 2:1), Zn^{2+} (7:1, 3.5:1), and Cd^{2+} (7:1).

The differences in NaOH consumption between pairs of titrations with and without Umpa were used in the calculations and the experimental data were collected every 0.1 pH unit in the pH range from 4.5 to a maximum of 10 (with Ca^{2+}). The data collection in the low pH range began when the degree of formation of the M(Umpa) complexes of about 2% was reached and the data collection in the upper pH range was terminated by the onset of the hydrolysis of $M(aq)^{2+}$; this hydrolysis was evident from the titrations without ligand.

In the calculation procedures we first took into account the species H^+, $H(Umpa)^-$, $Umpa^{2-}$, $(Umpa-H)^{3-}$, M^{2+}, M(Umpa), and $M(Umpa-H)^-$ and this led to the results assembled in Table 1 (Section 2.2). The curve fit was excellent in all instances, but chemical reasoning (see Section 2.4) and a slight dependence of $pK^{H}_{M(Umpa)}$ on the M^{2+} concentration in a few experiments also prompted us to include the $M_2(Umpa-H)^+$ species. However, the small concentration dependence indicated was always within the error limits and it did not allow values for the $M_2(Umpa-H)^-$ species to be calculated. Therefore, we calculated stability constants for these species, as described in Section 2.4, and by keeping these values constant we also took into account, aside from the species mentioned above, the formation of these $M_2(Umpa-H)^-$ species in the final calculations. The curve fits were excellent throughout and no dependence on the M^{2+} concentration was observed; these results are summarized in Table 3 (Section 2.4). It may be added that in many instances the error limits for $pK^{H}_{M(Umpa)}$ did indeed decrease somewhat (cf. the corresponding values in Table 1 and Table 3). The results given are the averages of at least four, on average six, independent pairs of titrations in each case.

4.3. Synthesis of di(isopropyl) 6-uracilmethylphosphonate (6Umpapr): 6-Chloromethyluracil and triisopropyl phosphite $[(CH_3)_2CHO]_3P$ were purchased from Sigma Aldrich. Melting points were determined with Boëtius apparatus. Microanalyses of C, H, and N were performed with a Perkin Elmer 2400 analyzer. Infrared spectra were recorded on an ALT Mattson Infinity Series FTIR spectrometer using KBr pellets. ^1H and ^{31}P NMR spectra were recorded on a Varian Mercury 300 spectrometer. Chemical shifts are reported using the standard (δ) notation in ppm with respect to TMS (1%) as an internal standard and H_3PO_4 (85%) as external standard. Triisopropyl phosphite was distilled immediately prior to use.

6-Chloromethyluracil (1.56 mmol, 0.25 g) was added portionwise to a solution of triisopropyl phosphite (20.27 mmol, 5 mL) by stirring under reflux until a transparent solution had formed. The course of the reaction was monitored by thin-layer chromatography. The solution was allowed to cool to room temperature followed by separation of the crystalline product, this was washed with ethanol and dried in vacuo to afford 6Umpapr as a white solid (0.21 g, 47%). M.p. 207–209 °C; ^1H NMR (300 MHz, DMSO): δ = 1.23 (dd, ^3J(H,H) = 8.63, 12H; $4CH_3$), 2.95 (d, ^2J(H,P) = 22.35, 2H; CH_2P), 4.58 (dq, ^3J(H,H) = 7.83, 2H; 2CH), 5.37 (d, ^4J(H,H) = 3.76, 1H; (aryl) H-C(5)), 10.75 (s, 1H; N(1)H), 11.02 ppm (s, 1H; N(3)H); ^{31}P NMR (300 MHz, $CDCl_3$): δ = 25.16 ppm; IR (KBr) $\tilde{\nu}_{max}$: (P-O-C) 983 (vs), (P=O) 1265 (vs), (C=O) 1724, 1649 (vs), (N-H) 2813–3099 cm^{-1} (vs, br); elemental analysis calcd (%) for $C_{11}H_{19}N_2PO_5$ (290.26): C 45.52, H 6.60, N 9.65; found: C 45.56, H 6.78, N 9.63.

4.4. Crystal structure determinations of 6Umpame and 6Umpapr: 6Umpame and 6Umpapr were recrystallized from ethanol, which yielded single crystals suitable for X-ray analysis. The diffraction data were collected on an Enraf-Nonius KappaCCD diffractometer.[39] Data reduction and cell refinement were performed by using the DENZO and SCALEPACK programs.[40] Structures were solved by direct methods[41] and refined by full-matrix least-squares methods based on F^2 by using the SHELXTL-PLUS[42] and SHELXL-97[43] programs. To resolve the ambiguity of the two possible rotamers, that is, assignment of C5 versus N1, both possibilities were tested and those resulting in the significantly lower final R values were chosen.

In 6Umpapr, all non-hydrogen atoms were refined anisotropically and hydrogen atoms were introduced at calculated positions with free refinement of the isotropic displacement factors. In 6Umpame, the large number of weakly observed reflections made it necessary to restrain some of the non-hydrogen atoms from anisotropic refinement, that is, the ring atoms N1 and C2, to save parameters and to attain a reflection-to-parameter ratio of at least 7:1 as required for noncentrosymmetric space groups and structures without heavy atoms. Coordinates and isotropic

Table 5. Crystal and refinement data for 6Umpame and 6Umpapr.

	6Umpame	6Umpapr
formula	$C_7H_{11}N_2O_5P$	$C_{11}H_{19}N_2O_5P$
formula weight	234.15	290.25
crystal system	orthorhombic	triclinic
space group	*Pbca*	$P\bar{1}$
a [Å]	7.383(1)	5.409(1)
b [Å]	14.118(3)	8.704(2)
c [Å]	19.250(4)	15.859(3)
α [°]	90	77.12(3)
β [°]	90	86.95(3)
γ [°]	90	89.12(3)
V [Å^3]	2006.5(7)	726.8(3)
Z	8	2
T [K]	293(2)	293(2)
λ [Å]	0.71073	0.71073
μ [mm^{-1}]	0.279	0.206
reflns collected	5618	2441
independent reflns (R_{int})	1650	1519
final R indices [$I>2\sigma(I)$]: R_1, wR_2[a]	0.0537, 0.1364	0.0478, 0.1014
final R indices (all data): R_1, wR_2[a]	0.1118, 0.1594	0.0894, 0.1127

[a] $R_1=\Sigma||F_o|-|F_c||/\Sigma|F_o|$, $wR_2=[\Sigma w(F_o^2-F_c^2)^2/\Sigma w(F_o^2)^2]^{1/2}$.

displacement factors of the hydrogen atoms were first refined freely until convergence of the structure and then fixed for the final cycles to save parameters. Details of the measurements and refinements are listed in Table 5.

CCDC-688406 and -688407 contain the supplementary crystallographic data for this paper. These data can be obtained free of charge from The Cambridge Crystallographic Data Centre via www.ccdc.cam.ac.uk/data_request/cif.

Acknowledgements

We thank Mrs. Astrid Sigel (Basel) for her competent help in the preparation of this manuscript and Mrs. Agnieszka Zdolska (Łódź) for her skillful help in the synthesis of 5Umpa and 6Umpa. Financial support from the Universities of Basel, Dortmund, Granada, and Zürich as well as from the Medical University of Łódź (grant nos. 503-3016-2 and 502-13-777 to J.O.), the Swiss National Science Foundation (SNF grant 20-113728/1 and SNF-Förderungsprofessur PP002-119106/1 to E.F.), the Deutsche Forschungsgemeinschaft (B.L.), the Fonds der chemischen Industrie (B.L.), a grant from the Deutscher Akademischer Austauschdienst (DAAD) to J.O., and a fellowship to C.F.M.-L. from the University of Granada are gratefully acknowledged.

[1] H. Sigel, *Pure Appl. Chem.* **1999**, *71*, 1727–1740.
[2] H. Sigel, *Chem. Soc. Rev.* **2004**, *33*, 191–200.
[3] J. Ochocki, J. Graczyk, *Pharmazie* **1998**, *53*, 884–885.
[4] K. Matlawska, U. Kalinowska, A. Erxleben, R. Osiecka, J. Ochocki, *Eur. J. Inorg. Chem.* **2005**, 3109–3117.
[5] A. Holý, *Curr. Pharm. Des.* **2003**, *9*, 2567–2592.
[6] *Chem. Rundsch. (1942–2002)* **2002**, issue no. *19*, p 68.
[7] http://www.emea.eu.int/humandocs/PDFs/EPAR/hepsera/610202en1.pdf
[8] R. Krejcova, K. Horska, I. Votruba, A. Holý, *Coll. Czech. Chem. Commun.* **2000**, *65*, 1653–1668.
[9] a) P. Barditch-Crovo, J. Toole, C. W. Hendrix, K. C. Cundy, D. Ebeling, H. S. Jaffe, P. S. Lietman, *J. Infect. Dis.* **1997**, *176*, 406–413; b) J.-P. Shaw, M. S. Louie, V. V. Krishnamurthy, M. N. Arimilli, R. J. Jones, A. M. Bidgood, W. A. Lee, K. C. Cundy, *Drug Metab. Dispos.* **1997**, *25*, 362–366.
[10] A. Holý, I. Votruba, M. Masojídková, G. Andrei, R. Snoek, L. Naesens, E. De Clercq, J. Balzarini, *J. Med. Chem.* **2002**, *45*, 1918–1929.
[11] H. Sigel, R. Griesser, *Chem. Soc. Rev.* **2005**, *34*, 875–900.
[12] C. F. Moreno-Luque, E. Freisinger, B. Costisella, R. Griesser, J. Ochocki, B. Lippert, H. Sigel, *J. Chem. Soc. Perkin Trans. 2* **2001**, 2005–2011.
[13] H. Sigel, C. P. Da Costa, B. Song, P. Carloni, F. Gregáň, *J. Am. Chem. Soc.* **1999**, *121*, 6248–6257.
[14] A. Fernández-Botello, R. Griesser, A. Holý, V. Moreno, H. Sigel, *Inorg. Chem.* **2005**, *44*, 5104–5117.
[15] B. Knobloch, C. P. Da Costa, W. Linert, H. Sigel, *Inorg. Chem. Commun.* **2003**, *6*, 90–93.
[16] B. Lippert, *Prog. Inorg. Chem.* **2005**, *54*, 385–447.
[17] Y. H. Jang, L. C. Sowers, T. Çağin, W. A. Goddard III, *J. Phys. Chem. A* **2001**, *105*, 274–280.
[18] R. K. O. Sigel, H. Sigel, *Met. Ions Life Sci.* **2007**, *2*, 109–180.
[19] C. F. Moreno-Luque, R. Griesser, J. Ochocki, H. Sigel, *Z. Anorg. Allg. Chem.* **2001**, *627*, 1882–1887.
[20] H. Sigel, D. B. McCormick, *Acc. Chem. Res.* **1970**, *3*, 201–208.
[21] H. Sigel, L. E. Kapinos, *Coord. Chem. Rev.* **2000**, *200–202*, 563–594.
[22] a) H. Irving, R. J. P. Williams, *Nature* **1948**, *162*, 746–747; b) H. Irving, R. J. P. Williams, *J. Chem. Soc.* 1953, 3192–3210.
[23] H. Sigel, B. Song, *Met. Ions Biol. Syst.* **1996**, *32*, 135–205.
[24] S. S. Massoud, H. Sigel, *Inorg. Chem.* **1988**, *27*, 1447–1453.
[25] H. Sigel, D. Chen, N. A. Corfù, F. Gregáň, A. Holý, M. Strašák, *Helv. Chim. Acta* **1992**, *75*, 2634–2656.
[26] H. Sigel, *Coord. Chem. Rev.* **1995**, *144*, 287–319.
[27] R. B. Martin, H. Sigel, *Comments Inorg. Chem.* **1988**, *6*, 285–314.
[28] B. Knobloch, W. Linert, H. Sigel, *Proc. Natl. Acad. Sci. USA* **2005**, *102*, 7459–7464.
[29] H. Sigel, S. S. Massoud, N. A. Corfù, *J. Am. Chem. Soc.* **1994**, *116*, 2958–2971.
[30] H. Sigel, R. B. Martin, *Chem. Rev.* **1982**, *82*, 385–426.
[31] B. Knobloch, H. Sigel, *J. Biol. Inorg. Chem.* **2004**, *9*, 365–373.
[32] H. Sigel, C. P. Da Costa, *J. Inorg. Biochem.* **2000**, *79*, 247–251.
[33] K. Aoki, *Met. Ions Biol. Syst.* **1996**, *32*, 91–134.
[34] K. Aoki, *J. Chem. Soc. Chem. Commun.* **1976**, 748–749.
[35] J. Deng, Y. Xiong, M. Sundaralingam, *Proc. Natl. Acad. Sci. USA* **2001**, *98*, 13665–13670.
[36] J. Ochocki, A. Erxleben, B. Lippert, *J. Heterocycl. Chem.* **1997**, *34*, 1179–1184.
[37] a) H. Sigel, A. D. Zuberbühler, O. Yamauchi, *Anal. Chim. Acta* **1991**, *255*, 63–72; b) M. Bastian, H. Sigel, *J. Coord. Chem.* **1991**, *23*, 137–154.
[38] a) C. A. Blindauer, T. I. Sjåstad, A. Holý, E. Sletten, H. Sigel, *J. Chem. Soc. Dalton Trans.* **1999**, 3661–3671; b) G. Kampf, L. E. Kapinos, R. Griesser, B. Lippert, H. Sigel, *J. Chem. Soc. Perkin Trans. 2* **2002**, 1320–1327.
[39] KappaCCD package, Nonius, Delft (The Netherlands), **1997**.
[40] DENZO and SCALEPACK: Z. Otwinowsky, W. Minor, *Methods Enzymol.* **1997**, *276*, 307–326.
[41] G. M. Sheldrick, *Acta Crystallogr. Sect. A* **1990**, *46*, 467–473.
[42] G. M. Sheldrick, SHELXTL-PLUS (VMS), Madison, WI (USA), **1990**.
[43] G. M. Sheldrick, SHELX-97, Program for Crystal Structure Refinement, University of Göttingen, Göttingen (Germany), **1997**.

Received: May 25, 2008
Published online: September 18, 2008

